Calibration of Pore Volume in Adsorption Experiments and Theoretical Models

Alexander V. Neimark*,†,‡ and Peter I. Ravikovitch‡

TRI/Princeton, Princeton, New Jersey 08542, and Department of Chemical Engineering, Yale University, New Haven, Connecticut 06520

Received March 10, 1997. In Final Form: June 30, 1997⊗

We propose a new definition of excess adsorption for use in molecular models of adsorption. This definition implies the calibration of theoretical models in a manner mimicking the experimental calibration procedure. The method of theoretical calibration is developed on the example of helium calibration. The notions of the He calibrated pore volume and the He calibrated pore size are introduced, and the He calibrated theoretical excess isotherms are defined. The proposed method diminishes the discrepancies between the theoretical and the experimental excess adsorption isotherms and makes the theory and the experiment entirely consistent. The quantitative estimates are made by means of the nonlocal density functional theory (NLDFT) applied to the adsorption of He, N_2, and CH_4 in micropores of active carbons at liquid nitrogen and ambient temperatures. It is shown that the experimental He calibration affects significantly the excess isotherms of vapors and supercritical fluids in microporous carbons. The nonmonotonous excess isotherms in molecular size pores are predicted. The theoretical predictions of He adsorption are in qualitative agreement with the experimental isotherm measured on the BPL active carbon at 77 K. The theoretical calibration is recommended for adjustment of any molecular model of adsorption phenomena, such as density functional theory, molecular dynamics, and grand canonical and other Monte Carlo simulations.

I. Introduction

Nanoporous materials with pores of width of several molecular diameters currently find numerous applications in modern technologies as adsorbents, catalysts, and host systems. Their engineering properties are determined primarily by their capability to specifically adsorb substances from bulk fluid phases. The practical problem of prediction of the adsorption properties of active carbons, zeolites, pillared clays, mesoporous molecular sieves, and many other traditional and newly synthesized adsorbents gave rise to a number of theoretical models capable of constructing adsorption isotherms in model pores.

Recent advances in molecular theories of inhomogeneous fluids have led to substantial progress in understanding the adsorption phenomena in nanopores. Modern methods of density functional theory (DFT), Monte Carlo simulations (MC), and molecular dynamics (MD) allow us to construct reference adsorption isotherms in model pores of a given geometry. In this paper, we address the general problem of correlation of the theoretical isotherms and the experimental data obtained by a particular technique.

The main issue is that, at present, the theoretical and the experimental definitions of adsorption isotherms are not entirely consistent: the theoretical isotherms deal initially with the absolute adsorption, which accounts for the total amount of adsorbate molecules residing in pores under given thermodynamic conditions, while the experimental isotherms deal inevitably with the excess adsorption resulting from a particular calibration procedure. As shown below, in the case of the molecular scale pores, the calibration may lead to substantial discrepancies between the experimental and the theoretical isotherms.

To remedy this situation, we propose to adjust the theory in order to make the theoretical results entirely consistent with the measurement results, namely to provide calibration of the theoretical model in the same manner as it would be done experimentally. The method of theoretical calibration proposed here is relevant to any theoretical model (DFT, MC, MD, *etc.*) and any experimental procedure. However, to be specific, we report quantitative conclusions based on the nonlocal DFT, as a theoretical method, and on the helium calibration, as the most widespread experimental calibration procedure. The adsorption of subcritical nitrogen and supercritical methane in pores of active carbons provides an example of practical systems. Experiments on helium adsorption on a sample of BPL active carbon were performed to demonstrate the practical importance of the proposed theoretical calibration.

The paper is organized as follows. In section II, we discuss the origins of the inconsistency of the theoretical and the experimental definitions of the excess adsorption. We show that there are two causes of this inconsistency: the ambiguousness in the theoretical setting of the pore boundaries and the experimental calibration of pore volume. The He calibration is considered in detail. In section III, we introduce the idea of calibration of theoretical models. We define the He calibrated pore volume and propose to use the He calibrated pore volume as a reference fluid volume while defining the theoretical excess isotherm. This definition of the He calibrated excess adsorption has two principal advantages: it is independent of the pore boundary settings, and it is consistent with the experimental excess adsorption. The notion of the He pore width is introduced for the slit-shaped pores. The effect of He calibration is evaluated first in the Henry approximation (section IV.1) and then by means of nonlocal density functional theory (section IV.2). Intermolecular potentials used for quantitative estimates are discussed in section IV.3. The He adsorption in model micropores of active carbons at nitrogen (77 K) and ambient temperatures is calculated in section V. It is shown that the helium adsorption at 77 K is significant in the sub-nanometer pores and that the He calibrated pore width determined at 77 K is a nonmonotonous function of the internal pore width with a prominent maximum in the range of molecular sizes. Conditions of

* Author for correspondence. E-mail: aneimark@triprinceton.org.
† TRI/Princeton.
‡ Yale University.
⊗ Abstract published in *Advance ACS Abstracts,* August 15, 1997.

S0743-7463(97)00266-7 CCC: $14.00

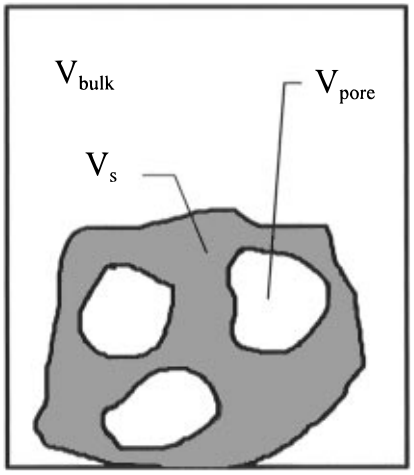

Figure 1. Solid−gas thermodynamic system.

the Boyle point are analyzed. The He calibrated excess isotherms of nitrogen are discussed in section VI.1. Isotherms in the sub-nanometer pores are shown to be nonmonotonous. In section VI.2, it is discussed how the He calibration affects the results of nitrogen adsorption porosimetry. The adsorption of methane at ambient temperature in the micropores of carbon is presented as an example of supercritical adsorption in section VI.3. In section VII, we present the experimental data on He adsorption at 77 K on the BPL active carbon to confirm our theoretical predictions. In the Conclusions, we summarize the results of the study and suggest the use of the He calibration of theoretical models for quantitative comparison of the experimental and the theoretical isotherms and for the elaboration of new methods for micropore characterization.

II. Origins of the Inconsistency of the Theoretical and Experimental Definitions of Excess Adsorption

II.1. Absolute and Excess Adsorption. The problem of correlation of the absolute and the excess adsorption dates back to Gibbs[1,2] (for a modern review, see ref 3). Classical interfacial thermodynamics operates exclusively with *excess* thermodynamic quantities defined with respect to a particular reference system, which consists of equilibrium bulk homogeneous phases bounded by *mathematical surfaces*. Let us consider a porous solid in equilibrium with a fluid (gas or liquid) (Figure 1). As a result of adsorption, the fluid at solid−fluid interfaces and in pores is inhomogeneous. To construct a reference system of homogeneous phases, it is necessary to set the solid−fluid boundary and thereby to define the phase volumes. In the rigorous thermodynamics of fluid adsorption on solid surfaces, the fluid−solid boundary is set provided that the excess mass/volume of the solid equals zero. That is, the total volume of a two-phase solid−fluid system is given as the sum of a reference solid volume and a reference fluid volume:

$$V_{sys} = V_s + V_f \tag{1}$$

provided that the reference solid volume, V_s, equals the ratio of the mass, M_s, of the solid to its density, ρ_s:

$$V_s = M_s/\rho_s \tag{2}$$

Basically, this implies the definition of the reference fluid volume, V_f,

$$V_f = V_{sys} - M_s/\rho_s \tag{3}$$

and of the excess adsorption, N_{ex}, which is defined as the difference between the total mass or number of fluid molecules, N_f, in the system and the number of molecules which would occupy the reference fluid volume V_f with the uniform density, ρ_f, of the equilibrium bulk fluid:

$$N_{ex} = N_f - \rho_f V_f \tag{4}$$

The reference fluid volume includes not only the pore volume V_{pore} inside the porous solid but also the volume of the bulk fluid V_{bulk} outside:

$$V_f = V_{pore} + V_{bulk} \tag{5}$$

Note that it is impossible to distinguish between these two volumes unless the porosity or pore geometries are known, and this is why one cannot define the absolute adsorption, which would account for all adsorbate molecules in pores:

$$N_{abs} = N_f - \rho_f V_{bulk} = N_{ex} + \rho_f V_{pore} \tag{6}$$

However, knowledge of porosity is not required while defining the excess adsorption by eq 4, which does not depend on the bulk fluid volume (increasing the bulk volume by ΔV_{bulk} implies increasing the total amount of adsorbate in the system by $\rho_f \Delta V_{bulk}$ and does not change the excess adsorption defined by eq 4). Thus, the classical interfacial thermodynamics deals with the excess adsorption only.

II.2. Calibration of Adsorption Experiments. Experimenters deal with the excess adsorption exclusively because it is not possible to separate the molecules confined in pores and the molecules in the equilibrium bulk phase. In the vast majority of experiments, the excess adsorption isotherms are calculated from eq 4 with the reference fluid volume, determined by means of a particular calibration procedure as the system volume, which is accessible to the adsorbate under given conditions. The rigorous thermodynamic definition (eq 3), which employs the density, ρ_s, of the solid phase, is rarely used in practice because the values of ρ_s are known for very special porous systems of regular structure only. In modern automated adsorption instruments, the calibration is the first standard step in the measurement procedure.

Calibration allows us to avoid uncertainties in the solid density and to introduce the excess adsorption isotherms in a regular manner. However, the experimental excess adsorption does not imply that the absolute adsorption can be easily calculated from eq 6 because the pore volume or porosity is not known beforehand. Determination of the porosity is one of the goals of adsorption experiments. Basically, the theoretical excess adsorption and the experimental excess adsorption are inevitably different. This discrepancy has been repeatedly discussed in the literature as related to the calibration of adsorption experiments. Numerous efforts have been made to analyze and diminish experimental uncertainties associated with calibration,[4] to convert the experimental excess adsorption into the absolute adsorption,[5,6] and to measure

(1) Gibbs, J. W. *Trans. Connect. Acad.* **1876**, *3*, 108; **1878**, *3*, 343.
(2) Gibbs, J. W. *The collected works*; Longmans, Green and Co.: 1928.
(3) Adamson, A. W. *Physical Chemistry of Surfaces*; Wiley: New York, 1982.
(4) Menon, P. G. *Chem. Rev.* **1968**, *68*, 277.
(5) Serpinski, V. V.; Pribylov, A. A.; Jakubov, T. S. *Izv. Akad. Nauk, Ser. Khim.* **1993**, 1150.

the absolute adsorption in systems with a known porosity such as zeolites.[7]

Calibration implies the measurement of the amount of a presumably nonadsorbing gas in the system containing a given porous sample. In volumetric and gravimetric adsorption measurements, the reference fluid volume V_f in the adsorption system is usually determined by means of helium.[8,9] It is recommended to perform the He calibration at "as high a temperature as convenient".[9]

Use of He for calibration of the adsorption volume and determining the true density of porous solids dates back to Washburn.[10] In most of experimental measurements, the He calibration is performed either at the temperature of the adsorption experiment (77 K, in the case of nitrogen adsorption to be measured[11]) or at room temperature (in the case of adsorption at ambient or higher temperatures to be measured). The total amount of He in the adsorption system, $N_{f,He}$, is measured at a given temperature T_{cal} and pressure P_{cal}, and the reference fluid volume is defined as

$$V_{f,He} = N_{f,He}(T_{cal},P_{cal})/\rho_{f,He}(T_{cal},P_{cal}) \qquad (7)$$

Here, $\rho_{f,He}$ is the density of bulk helium under these conditions. This definition implies that the excess adsorption of He, defined by eq 4, equals zero. This in no way means that He is not adsorbed at the pore walls, and its density is homogeneous within the pores. In fact, eq 7 is a legitimate method for introducing the reference system, which is based on the requirement that the excess mass of fluid (He) equals zero. It is an alternative to the rigorous method discussed above, which required zero excess mass of solid. The reference fluid volume as defined by the He calibration includes contributions from the bulk volume outside the sample and the pore volume inside the sample, $V_{f,He} = V_{pore,He} + V_{bulk}$. Here, we use the additional subscript "*He*" in $V_{pore,He}$ to emphasize that the pore volume appearing in the He calibration may (and as we will show below does) differ from the geometrical pore volume appearing in the theory. While using the He calibration, the sum of the solid volume (eq 2) and the reference fluid volume (eq 7) does not have to be equal to the system volume (eq 1). The definitions in eqs 3 and 7 would be consistent only if He was not physically adsorbed at the solid surface.

Thus, as the result of the He calibration, the experimental excess adsorption is defined as

$$N_{ex}^{exp} = N_f^{exp} - (\rho_f/\rho_{f,He})N_{f,He} \qquad (8)$$

where N_f^{exp} is the experimentally determined total amount of adsorbate molecules in the system, both in the pore volume, V_{pore}, and in the bulk volume, V_{bulk}.

The He calibration is reasonable only if the ratio $N_{f,He}/\rho_{f,He}$ is a constant within a sufficiently wide range of pressures that is correct for most of the systems. However, even when $N_{f,He}$ and $\rho_{f,He}$ are proportional, the He adsorption may occur. The He adsorption leads to an overestimation of the pore volume and an underestimation of the measured excess adsorption isotherms. The magnitude of this error depends on the material and on the temperature at which He calibration is performed.

The fact that highly porous materials do adsorb He even at ambient temperature is well-known; see, *e.g.*, refs 4 and 12−14. He adsorption at low temperature (4 K) is proposed as a routine method for characterization of microporous materials.[15] Adsorption of helium on carbonaceous materials at higher temperatures (>70 K) has been extensively used for determination of the solid−gas virial coefficients and the parameters of the solid−gas potential by the method developed by Steele and Halsey.[16−19] For more references on this subject, see ref 20, p 314. Our experiments with He adsorption on a sample of active carbon BPL have shown that He adsorption in micropores is appreciable and has to be taken into account while analyzing the excess adsorption isotherms obtained by using He calibration (see section VII).

We may conclude that the experimental excess adsorption isotherms defined by means of calibration are not consistent with the rigorous definition of excess adsorption (eqs 3 and 4) and do not allow calculations of the absolute adsorption isotherms. Now, let us consider what we encounter while modeling adsorption in pores.

II.3. Definitions of Excess Adsorption in Molecular Theories. Molecular theories (DFT, MC, MD, *etc.*) allow for calculation of the inhomogeneous density of adsorbate molecules, $\rho(\mathbf{r})$, in model pores of given geometry, which yields the absolute adsorption, N_{abs}, calculated as an integral of the density over the pore volume

$$N_{abs} = \int_V \rho(\mathbf{r})\, d\mathbf{r} \qquad (9)$$

The excess adsorption, N_{ex}, is defined as the difference between the absolute adsorption and the number of molecules which would occupy the reference pore volume with the uniform density of adsorbate in the equilibrium bulk phase:

$$N_{ex} = N_{abs} - \rho_f V_{pore,theor} \qquad (10)$$

The reference theoretical pore volume, $V_{pore,theor}$, depends on how the pore boundaries are set and does not necessarily coincide with the volume of integration in eq 9.

The ambiguousness of the pore boundary settings has been repeatedly discussed in the literature; see, *e.g.*, ref 21. Let us consider a different way to set the pore boundary on the example of a slitlike pore between two graphite surfaces, as illustrated in Figure 2. In this simplest case, the reference pore volume, $V_{pore,theor} = HS$, where H is the pore width, which requires a special definition, and S is the area of one graphite surface, which is supposed to be sufficiently large, $\sqrt{S} \gg H$. In such a pore, the adsorbate molecules are subject to the adsorbate−adsorbent poten-

(6) Serpinski, V. V.; Jakubov, T. S. *Izv. Akad. Nauk, Ser. Khim.* **1985**, 12; *Adv. Sci. Technol.* **1993**, *10*, 85.
(7) Pribylov, A. A.; Serpinsky, V. V.; Kalashnikov, S. M. *Zeolites* **1991**, *11*, 846.
(8) Sing, K. S. W.; Everett, D. H.; Haul, R. A. W.; Moscou, L.; Pierotti, R. A.; Rouquerol, J.; Siemieniewska, T. *Pure Appl. Chem.* **1985**, *57*, 603.
(9) Rouquerol, J.; Avnir, D.; Fairbridge, C. W.; Everett, D. H.; Haynes, J. H.; Pernicone, N.; Ramsay, J. D. F.; Sing, K. S. W.; Unger, K. K. *Pure Appl. Chem.* **1994**, *66*, 1739.
(10) Washburn, E. W.; Buntung, E. N. *J. Am. Ceram. Soc.* **1922**, *5*, 112.
(11) Olivier, J. P. *AIChE Topical Conference "Recent Developments and Future Opportunities in Separation Technology"*, Nov 12−17, 1995; AIChE: Miami, FL; Vol. 2, p 162.
(12) Maggs, F. A. P.; Schwabe, P. H.; Williams, J. H. *Nature* **1960**, *186*, 956.
(13) Hellemans, R.; Van Itterbeek, A.; Van Deal, W. *Physica* **1967**, *34*, 429.
(14) Suzuki, I.; Kakimoto, K.; Oki, S. *Rev. Sci. Instrum.* **1987**, *58*, 1226.
(15) Setoyama, N.; Ruike, M.; Kasu, T.; Suzuki, T.; Kaneko, K. *Langmuir* **1993**, *9*, 2612.
(16) Steele, W. A.; Halsey, G. D., Jr. *J. Chem. Phys.* **1954**, *22*, 979.
(17) Steele, W. A.; Halsey, G. D., Jr. *J. Phys. Chem.* **1955**, *59*, 57.
(18) Freeman, M. P. *J. Phys. Chem.* **1958**, *62*, 723.
(19) Constabaris, G.; Singleton, J. H.; Halsey, G. D., Jr. *J. Phys. Chem.* **1959**, *63*, 1350.
(20) Steele, W. A. In *The Solid−Gas Interface*; Flood, E. A., Ed.; Marcel Dekker: New York, 1967; Vol. 1.
(21) Kaneko, K.; Cracknell, R. F.; Nicholson, D. *Langmuir* **1994**, *10*, 4606.

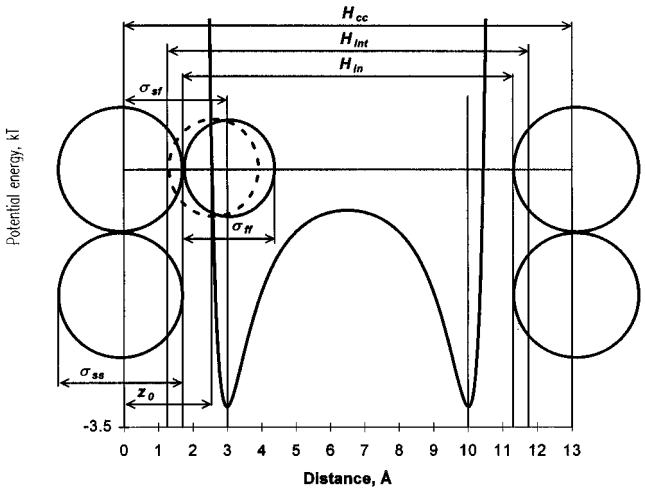

Figure 2. Various definitions of the pore size on the example of He in a carbon slit pore. 10-4-3 potential of Steele. He−carbon parameters were taken from combining rules (see text).

tial induced by the graphite surfaces. In nanopores, the potentials from opposite walls may overlap, and the overall adsorbate−adsorbent potential is commonly presented as the sum of the two graphite surface potentials:

$$U_{sf,pore}(z) = U_{sf}(z) + U_{sf}(H_{cc} - z) \tag{11}$$

Here, H_{cc} is the distance between the plane of atom centers in the first graphitic layer on one wall, where the origin of the z-coordinate is set, and the plane of atom centers in the first graphitic layer on the opposite wall. This distance characterizes the pore width and sometimes is used as a nominal pore size (ref 20, p 318). This definition of the pore width is convenient from the point of view of molecular modeling yet inconsistent with the rigorous thermodynamic setting of the fluid−solid boundary because it does not provide the zero excess mass/volume of the solid. Technically, the pore volume, proportional to H_{cc}, can be used as the reference fluid volume while defining the excess adsorption through eq 10. However, this volume obviously exceeds the physical volume available for adsorbate molecules.

To fulfill the zero solid mass/volume excess requirement, one should set the pore boundaries at the edges of the external graphitic layers and use as the internal pore width

$$H_{in} = H_{cc} - \Delta \tag{12}$$

where $\Delta = 3.35$ Å is the interlayer spacing in graphite. Intuitively, the internal pore width H_{in} seems to be the most suitable pore size for defining the reference pore volume, $V_{pore,theor}$, in the excess adsorption equation (eq 8).

Sometimes, instead of the interlayer spacing, the Lennard-Jones diameter of the carbon atom, σ_{ss}, is used. For carbon $\sigma_{ss} = 3.4$ Å;[22] this leads to a minor difference (0.05 Å) in the internal pore width H_{in}, defined as

$$H_{in} = H_{cc} - \sigma_{ss} \tag{13}$$

Note that both these definitions (eqs 12 and 13) are independent of the adsorbate and the temperature.

However, Kaneko *et al.*[21] argued that this definition ignored the fact that the distance of the closest approach of the adsorbate molecules to the solid should be determined by the adsorbate−adsorbent interaction potential, $U_{sf}(z)$. Because the distance of the closest approach of the adsorbate molecules to the wall equals the distance at which the adsorbate−adsorbent interaction potential, $U_{sf}(z)$, passes through zero, z_0, they suggested that the internal pore width should be defined as

$$H_{int} = H_{cc} - 2z_0 + \sigma_{ff} \tag{14}$$

where σ_{ff} is the Lennard-Jones diameter of the adsorbate molecule and z_0 is reckoned from the outer carbon atom centers to the adsorbate molecule centers. The value of z_0 depends on the form of the solid−fluid potential. Consider the 10-4-3 potential of Steele,[22] which is widely used for modeling the interactions of simple molecules with graphite:

$$U_{sf}(z) = 2\pi\rho_s\epsilon_{sf}\sigma_{sf}^2\Delta\left[\frac{2}{5}\left(\frac{\sigma_{sf}}{z}\right)^{10} - \left(\frac{\sigma_{sf}}{z}\right)^4 - \frac{\sigma_{sf}^4}{3\Delta(0.61\Delta + z)^3}\right] \tag{15}$$

where $\rho_s = 0.114$ Å^{-3} is the density of solid atoms and ϵ_{sf} and σ_{sf} are the energetic and scale parameters of the solid−fluid Lennard-Jones potential. For this potential, the distance of closest approach $z_0 = 0.8506\sigma_{sf}$ (Figure 2). Thus, the difference in the internal pore widths, defined by eqs 12 and 14, is about 0.1 nm.[21] The nominal and the internal pore widths, H_{cc} and H_{in} (or H_{int}), differ by about one molecular diameter, about 0.3 ± 0.04 nm.

These differences in the assigned pore sizes may not be essential while calculating the theoretical excess isotherms of subcritical fluids, when the bulk density is sufficiently low. However, they may lead to an appreciable difference in the calculated excess adsorption isotherms in the case of the micropores of size of a few molecular diameters while considering adsorption of supercritical fluids. The pore width definition affects the pore size distributions calculated from comparison of the experimental and the theoretical isotherms. The smaller the pore, the larger the discrepancy expected. We note that the absolute adsorption (eq 9), calculated by integrating the density profile, is insensible to the pore boundary settings because in any event the density vanishes at the distance less than half of the molecular diameter from the centers of solid molecules (assuming that $z_0 > 0.5\sigma_{sf}$).

The above-mentioned ambiguousness in the definition of the theoretical pore size is not the only source of the inconsistency between the theoretical and the experimental excess isotherms. The major factor is that the theoretical definitions are based on purely geometrical considerations while the experimental definition of the excess adsorption does not involve any pore geometries. The reference fluid volume is evaluated experimentally by means of a particular calibration procedure as the system volume accessible to probe molecules (e.g., He) under given conditions.

We conclude that the theory and experiment are not consistent, and the theoretical excess adsorption and the experimental excess adsorption are inevitably different.

In this paper, we propose a new method for defining the theoretical excess isotherms, which makes the theoretical results entirely consistent with the experimental ones. Namely, we propose to provide the calibration of a theoretical model in use in the same manner as would be done in the experiment and thereby to get around the inevitable experimental difficulties.

III. He Calibration of Model Pores

If the volume of a model pore were appraised by means of the He calibration, one would obtain

(22) Steele, W. A. *The Interactions of Gases with Solid Surfaces*; Pergamon: New York, 1974.

$$V_{\text{pore,He}} = N_{\text{abs,He}}/\rho_{\text{f,He}} = \int_V \rho_{\text{He}}(\mathbf{r})\, d\mathbf{r}/\rho_{\text{f,He}} \quad (16)$$

The total amount of He molecules in the pore, or the absolute He adsorption, $N_{\text{abs,He}}$, can be predicted by using the same theoretical method which is employed for calculating the adsorption of the adsorbate under consideration. To determine the "helium calibrated" pore volume, one has to calculate the He density, $\rho_{\text{He}}(\mathbf{r})$, based on the He−He and He−solid intermolecular potentials and to integrate the He density, $\rho_{\text{He}}(\mathbf{r})$, over the pore volume. This density should not be necessarily a homogeneous one and may differ from the bulk density of He, $\rho_{\text{f,He}}$, at the pore walls.

We propose to use the "helium calibrated" pore volume as a reference fluid volume while defining the theoretical excess isotherm:

$$N_{\text{ex}} = N_{\text{abs}} - \rho_{\text{f}} V_{\text{pore,He}} = N_{\text{abs}} - \frac{\rho_{\text{f}}}{\rho_{\text{f,He}}} N_{\text{abs,He}} = \int_V \rho(\mathbf{r})\, d\mathbf{r} - \frac{\rho_{\text{f}}}{\rho_{\text{f,He}}} \int_V \rho_{\text{He}}(\mathbf{r})\, d\mathbf{r} \quad (17)$$

In other words, the "helium calibrated" pore volume is the volume that holds a number of moles of helium at its *bulk* density which is equivalent to the amount found in the pore at the *actual* adsorbed helium density.

This definition of the excess adsorption has two principal advantages: it is independent of the pore boundary settings, and it is consistent with the experimental excess adsorption.

On the basis of the theoretical He calibration, one can introduce, together with the "helium calibrated" pore volume, the "helium calibrated" pore size, or shortly the He pore size. For the slit-shaped pore discussed above (Figure2), the He pore width is defined as

$$H_{\text{He}} = \int_0^H \rho_{\text{He}}(z)\, dz/\rho_{\text{f,He}} \quad (18)$$

The He pore width is the width of the effective slit-shaped pore having the "helium calibrated" pore volume. In terms of the He pore width, the He calibrated excess isotherm (eq 17) in a slit-shaped pore is expressed as

$$N_{\text{ex}} = S\int_0^H \rho(z)\, dz - \rho_{\text{f}} S H_{\text{He}} \quad (19a)$$

The excess adsorption per unit area is written as

$$N^{\text{s}}_{\text{ex}} = \frac{1}{2}\left(\int_0^H \rho(z)\, dz - \rho_{\text{f}} H_{\text{He}}\right) \quad (19b)$$

The factor $^1/_2$ in eq 19b is due to the integration from 0 to H, which accounts for the contributions from both pore walls.

The discrepancy between the He pore width and the geometrical internal pore width reflects the effect of the He adsorption at the pore walls. One may expect that this effect is negligible for sufficiently wide pores yet appreciable for micropores. This is confirmed by the following analysis.

IV. Modeling of He Adsorption

IV.1. Henry Region. In the Henry region of sufficiently low densities, the equilibrium density profile is determined exclusively by the external potential of solid−fluid interactions:[20]

$$\rho(\mathbf{r}) = \rho_{\text{f}} \exp[-U_{\text{ext}}(\mathbf{r})/k_{\text{B}}T] \quad (20)$$

For He, which is commonly assumed as a nonadsorbing gas, this approximation seems to be reasonable as the first-order correction to account for its adsorption. The Henry law has been used for interpretation of experimental adsorption isotherms of He on different substrates.[13,14] Therewith, the absolute He adsorption in the pore equals

$$N_{\text{abs,He}} = \rho_{\text{f,He}} \int_V \exp[-U_{\text{ext,He}}(\mathbf{r})/k_{\text{B}}T]\, dV \quad (21)$$

The Henry approximation implies that the helium calibrated pore volume equals

$$V_{\text{pore,He}} = \int_V \exp[-U_{\text{ext,He}}(\mathbf{r})/k_{\text{B}}T]\, dV \quad (22)$$

and that the He pore size for the slit-shaped pore equals

$$H_{\text{He}} = \int_0^H \exp[-U_{\text{ext,He}}(z)/k_{\text{B}}T]\, dz \quad (23)$$

The deviations of $V_{\text{pore,He}}$ and H_{He} from the corresponding geometrical dimensions of the region of integration in eqs 22 and 23, V and H, are quantitative measures of He adsorbency. The excess He adsorption, defined by using the geometrical volume as the reference fluid volume, is expressed through the solid−gas second virial coefficient, $B_{\text{sg,He}}$,[20]

$$N_{\text{ex,He}} = \rho_{\text{f,He}} \int_V [\exp[-U_{\text{ext,He}}(\mathbf{r})/k_{\text{B}}T] - 1]\, d\mathbf{r} = \rho_{\text{f,He}} B_{\text{sg,He}} = \rho_{\text{f,He}}(V_{\text{pore,He}} - V) \quad (24)$$

which is equal to

$$B_{\text{sg,He}} = V_{\text{pore,He}} - V \quad (25)$$

In the slit geometry, the excess He adsorption per unit area (eq 19b) is written using the He pore width:

$$N^{\text{s}}_{\text{ex,He}} = \rho_{\text{f,He}} \frac{1}{2} \int_0^H [\exp[-U_{\text{ext,He}}(z)/k_{\text{B}}T] - 1]\, dz = \rho_{\text{f,He}} \frac{1}{2}(H_{\text{He}} - H) \quad (26)$$

In narrow pores, where the potentials from the opposite pore walls overlap, the excess He adsorption differs from the specific excess adsorption on an open surface

$$N^{\text{s}}_{\text{ex,He}} = \rho_{\text{f,He}} \int_0^\infty [\exp[-U_{\text{ext,He}}(z)/k_{\text{B}}T] - 1]\, dz \quad (27)$$

and, in general, depends on the pore dimension. In sufficiently wide pores without overlapping the pore wall potentials, the specific excess adsorption on an open surface (eq 27) is a good estimate.

Adsorption on an open surface can be characterized in terms of the solid−gas second virial coefficient, $B^{\text{s}}_{\text{sg,He}}$, having dimension of length,

$$B^{\text{s}}_{\text{sg,He}} = \int_0^\infty [\exp[-U_{\text{ext,He}}(z)/k_{\text{B}}T] - 1]\, dz \quad (28)$$

as

$$N^{\text{s}}_{\text{ex,He}} = B^{\text{s}}_{\text{sg,He}}\, \rho_{\text{f,He}} \quad (29)$$

The solid−gas second virial coefficient, $B^{\text{s}}_{\text{sg,He}}$, gives a simple criteria: the He adsorption at the pore walls can be disregarded only in pores substantially wider than $B^{\text{s}}_{\text{sg,He}}$. In pores narrower than $B^{\text{s}}_{\text{sg,He}}$, adsorption dominates and makes a major contribution to the total number

of molecules confined in the pore. Therewith, the He calibrated pore width, H_{He}, is greater than $B^s_{sg,He} + H$. The above considerations are valid in the case of positive $B^s_{sg,He}$. With the increase of temperature, the physical adsorption diminishes, and $B^s_{sg,He}$ is expected to decrease gradually and to get past zero. When $B^s_{sg,He}$ is of the order of molecular sizes, a clear setting of the pore boundaries is important.

This aspect of the He calibration has been discussed earlier by Steele.[20] Steele also noted that the pore size determined by He depends on the temperature (ref 20, p 319). Thus, the geometrical pore size would be obtained only at a certain temperature, where $B_{sg,He} = 0$. This temperature, referred to as the Boyle point, had been estimated to be about 290 K for sufficiently wide pores of carbons. Note that, while making these estimates, Steele reckoned the distance from the atom centers of the outer carbon layer and considered the nominal pore width H_{cc} as the geometrical pore width in the definition of the excess adsorption. The use of the Boyle point in adsorption studies is discussed further in section V.3.

When adsorption of a given adsorbate also follows the Henry law, the "helium calibrated" excess isotherm can be expressed in a symmetric form:

$$N_{ex} = N_{abs} - \rho_f V_{pore,He} = \rho_f \int_V [\exp[-U_{ext}(\mathbf{r})/k_B T] - \exp[-U_{ext,He}(\mathbf{r})/k_B T_{cal}]]\, d\mathbf{r} \quad (30)$$

Equation 30 in the case of the slit-shaped geometry is rewritten as

$$N_{ex} = \rho_f S \int_0^H [\exp[-U_{ext}(z)/k_B T] - \exp[-U_{ext,He}(z)/k_B T_{cal}]]\, dz \quad (31)$$

Equations 30 and 31 may be useful for estimating adsorption at low pressures.

In the general case, the adsorbate density cannot be expressed in terms of the Henry equation, and provided that the He calibration is carried out in the Henry region (as shown below, this is the case in most of the experimental measurements), the He calibrated excess adsorption equals

$$N_{ex} = \int_V [\rho(\mathbf{r}) - \rho_f \exp[-U_{ext,He}(\mathbf{r})/k_B T_{cal}]]\, d\mathbf{r} \quad (32)$$

and in the slit-shaped pore

$$N_{ex} = S\int_0^H \rho(z)\, dz - \rho_f S \int_0^H \exp[-U_{ext,He}(z)/k_B T_{cal}]\, dz = S\int_0^H \rho(z)\, dz - \rho_f S H_{He} \quad (33)$$

IV.2. Nonlocal Density Functional Theory. Quantitative analyses of the significance of the proposed calibration of the theoretical isotherms have been performed on the basis of Tarazona's version[23] of the nonlocal density functional theory (NLDFT), known as a smoothed density approximation (SDA) (for review, see *e.g.* ref 24) with examples of adsorption of He at 77 and 308 K, N_2 at 77 K, and CH_4 at 308 K in model slit-shaped micropores of active carbons. This model has been widely employed previously and is proven to be effective for predicting adsorption of simple molecules in micro- and mesopores.[25−32]

The density $\rho(\mathbf{r})$ of adsorbate confined in a pore at given chemical potential μ and temperature T is determined by minimization of the grand thermodynamic potential (GP). In the NLDFT, the GP is expressed as the functional of the local fluid density $\rho(\mathbf{r})$ in the following form:

$$\Omega[\rho(\mathbf{r})] = \int d\mathbf{r}\, \rho(\mathbf{r})[k_B T(\ln(\Lambda^3\rho(\mathbf{r})) - 1) + f_{ex}(\bar{\rho}(\mathbf{r}))] + \frac{1}{2}\int\int d\mathbf{r}\, d\mathbf{r}'\, \rho(\mathbf{r})\, \rho(\mathbf{r}')\, \Phi_{attr}(|\mathbf{r}-\mathbf{r}'|) - \int d\mathbf{r}\, \rho(\mathbf{r})[\mu - U_{ext}(\mathbf{r})] \quad (34)$$

Here, $U_{ext}(\mathbf{r})$ is the external solid−fluid potential imposed by the pore walls and $\Phi_{attr}(r)$ is the attractive part of the fluid−fluid potential. By varying the parameters of these potentials, one can consistently describe adsorption of different species. Λ denotes the de Broglie thermal wavelength in the ideal gas term. The excess Helmholtz free energy of the reference hard sphere fluid, $f_{ex}(\bar{\rho}(\mathbf{r}))$, is calculated from the Carnahan−Starling equation of state.[33] The SDA implies that $f_{ex}(\bar{\rho}(\mathbf{r}))$ depends on the smoothed density $\bar{\rho}(\mathbf{r})$ defined as

$$\bar{\rho}(\mathbf{r}) = \int d\mathbf{r}'\, \rho(\mathbf{r}')\, \omega(|\mathbf{r}-\mathbf{r}'|,\bar{\rho}(\mathbf{r})) \quad (35)$$

where the weighting function $\omega(|\mathbf{r}-\mathbf{r}'|)$ was chosen to reproduce the Percus−Yevick approximation of the direct correlation function of the homogeneous hard-sphere fluid.[23]

The minimization of the grand potential by the method of indeterminate Lagrange multipliers (ILM)[34] yields the following equation for the density profile $\rho(\mathbf{r})$

$$\mu = k_B T \ln(\rho(\mathbf{r})\Lambda^3) + f_{ex}(\bar{\rho}(\mathbf{r})) - \int d\mathbf{r}'\, \lambda(\mathbf{r}')\, \omega(|\mathbf{r}-\mathbf{r}'|,\bar{\rho}(\mathbf{r}')) + U_{ext}(\mathbf{r}) + \int d\mathbf{r}'\, \rho(\mathbf{r}')\, \Phi_{attr}(|\mathbf{r}-\mathbf{r}'|) \quad (36)$$

with the ILM function

$$\lambda(\mathbf{r}) = -\rho(\mathbf{r})\, f'_{ex}(\mathbf{r}) \Big/ \left[1 - \int d\mathbf{r}'\, \rho(\mathbf{r}')\, \frac{d\omega(|\mathbf{r}-\mathbf{r}'|,\bar{\rho}(\mathbf{r}))}{d\bar{\rho}(\mathbf{r})}\right] \quad (37)$$

Note that, at low densities, the gas−gas interactions are negligible, and with the chemical potential of an ideal gas, $\mu = k_B T \ln(\rho_g \Lambda^3)$, eq 36 degenerates into eq 20.

IV.3. Potentials of Intermolecular Interactions. The Lennard-Jones 6−12 potential was used to model

(23) Tarazona, P. *Phys. Rev. A* **1985**, *31*, 2672. Tarazona, P.; Marini Bettolo Marconi, U.; Evans, R. *Mol. Phys.* **1987**, *60*, 573.
(24) Evans, R. In *Fundamentals of Inhomogeneous Fluids*; Henderson, D., Ed.; Marcel Dekker: New York, 1992.
(25) Lastoskie, C.; Gubbins, K. E.; Quirke, N. *J. Phys. Chem.* **1993**, *97*, 4786.
(26) Lastoskie, C.; Gubbins, K. E.; Quirke, N. *Langmuir* **1993**, *9*, 2693.
(27) Olivier, J. P.; Conklin, W. B.; von Szombathely, M. In *Charact. Porous Solids 3* **1994**, *87*, 81. Olivier, J. P. *J. Porous Mater.* **1995**, *2*, 217.
(28) Ravikovitch, P. I.; Ó Domhnaill, S. C.; Neimark, A. V.; Schüth, F.; Unger, K. K. *Langmuir* **1995**, *11*, 4765.
(29) Neimark, A. V.; Ravikovitch, P. I.; Ó Domhnaill, S. C.; Schüth, F.; Unger, K. K. In *Fundamentals of Adsorption*; LeVan, M. D., Ed.; Kluwer: Boston, 1996; p 667.
(30) Neimark, A. V.; Ravikovitch, P. I.; Grün, M.; Schüth, F.; Unger, K. K. *Character. Porous Solids 4*, in press.
(31) Ravikovitch, P. I.; Wei, D.; Chueh, W. T.; Haller, G. L.; Neimark, A. V. *J. Phys. Chem. B* **1997**, *101*, 3671.
(32) Balbuena, P. B.; Gubbins, K. E. *Langmuir* **1993**, *9*, 1801.
(33) Carnahan, N. F.; Starling, K. E. *J. Chem. Phys.* **1969**, *51*, 635.
(34) Neimark, A. V. *Langmuir* **1995**, *11*, 4183.

Table 1. Parameters of the Intermolecular Potentials Used in Calculations

gas	ϵ_{ff}/k_B, K	σ_{ff}, Å	d_{HS}, Å	ref	ϵ_{sf}/k_B, K	σ_{sf}, Å	ref
He	10.41	2.602	2.55	36	15	2.98	37
N_2	94.45	3.575	3.575	28	53.22	3.494	25
CH_4	148.1	3.81	3.81	22	64.4	3.605	combining rules

fluid−fluid interactions. The attractive interactions were modeled using the Weeks−Chandler−Andersen (WCA) perturbation scheme:[35]

$$\Phi_{attr}(r) = \begin{cases} -\epsilon_{ff}, & r < r_m \\ \Phi_{ff}(r), & r_m < r < r_c \\ 0, & r > r_c \end{cases} \quad (38)$$

where $\Phi_{ff}(r)$ is the fluid−fluid intermolecular potential, ϵ_{ff} is the potential well-depth, $r_m = 2^{1/6}\sigma_{ff}$ is the distance of the minimum of the potential well, and r_c is a cutoff distance.

Parameters of the LJ fluid−fluid potentials of the adsorbates used in this study are listed in Table 1. In addition to the LJ collision diameter, σ_{ff}, the NLDFT employs the equivalent hard sphere diameter, d_{HS}, in the Carnahan−Starling equation of state. The latter is not supposed to be necessarily equal to σ_{ff}, and it serves as an adjustable parameter to provide the best fit to the experimental bulk fluid properties. The equivalent hard sphere diameter of N_2 was taken from our previous work.[28] The equivalent hard sphere diameter of CH_4 was set equal to σ_{ff}. For He, the equivalent hard sphere diameter, d_{HS}, was chosen to be slightly smaller than σ_{ff}, namely 2.55 Å, to ensure that at 77 K the theory predicts the same bulk pressures as given by the virial equation of state. Quantum corrections for He were not considered. According to Derderian and Steele,[38] the quantum-mechanical second virial coefficient of Lennard-Jones He^4 at 77 K is ca. 20 % bigger than the classical one, which itself is a small value.

The solid−fluid interactions of the gases with the pore walls in active carbons were modeled by the 10-4-3 potential of Steele (eq 15), and the external solid−fluid potential in the slit-shaped geometry was calculated as given by eq 11. The LJ solid−fluid interaction parameters used in calculations are presented in Table 1. Parameters of the C−He interactions were taken as recommended by Steele.[37] We have also performed calculations with the C−He parameters obtained from the combining rules and with the parameters recommended by Vidali and Cole.[39] We found that He adsorption strongly depends on the chosen set of parameters, but among three different sets of parameters, those recommended by Steele give an averaged effect of He adsorption. Also, adsorption isotherms calculated with these parameters agree well with our experimental measurements of He adsorption on BPL carbon. Thus, all calculations presented in this paper were performed with the C−He parameters recommended by Steele. For C−N_2 interactions we used parameters recommended by Lastoskie *et al.*;[25] and the C−CH_4 parameters were obtained from the combining rules, using for carbon $\epsilon_{cc} = 28$ K and $\sigma_{cc} = 3.4$ Å.[22]

V. Calculations of He Adsorption in the Model Pores

The He adsorption isotherms in the slit-shaped pores of active carbons were calculated by means of the NLDFT model described above at 77 and 308 K. To demonstrate the effect of confinement in the pores of different sizes, the results are presented as the absolute adsorption per unit of pore volume (average density):

$$\bar{\rho} = N/V_{pore,geom} = \frac{1}{H_{in}}\int_0^{H_{cc}} \rho(z)\, dz = \frac{H_{He}}{H_{in}}\rho_{f,He} \quad (39)$$

Here, the internal pore width is represented by $H_{in} = H_{cc} - \sigma_{ss}$ (eq 13), and the average density in the pore is proportional to the He pore width, H_{He}, defined by eq 18.

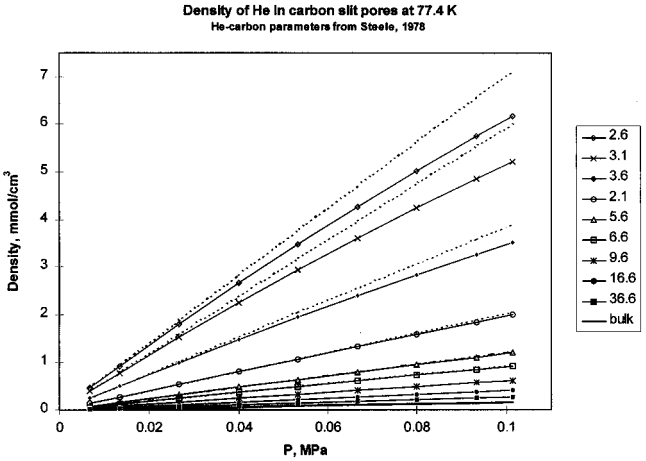

Figure 3. NLDFT absolute adsorption isotherms of He in carbon micropores at 77.4 K. The density of He has been calculated from eq 39. Dotted lines are Henry isotherms. Pore sizes are internal, H_{in}.

V.1. He Adsorption at 77.4 K. At 77.4 K, the solid−gas second virial coefficient (eq 28), $B^s_{sg,He}$, was estimated as 11.9 Å. Therefore, one can expect an appreciable effect of He adsorption at the carbon surface at 77 K in micropores narrower than ca. 10 Å.

This conclusion is confirmed by the NLDFT calculations. The average densities of He in pores of different widths are presented in Figure 3. The dependence of He adsorption on the pore size is not monotonous. The smallest pore considered ($H_{in} = 2.1$ Å) is too narrow even for a He molecule, and adsorption is lower than in wider micropores. In the micropores of molecular sizes, adsorption increases, and the calculated average density exceeds the bulk density by up to 39 times at atmospheric pressure and 45 times in the Henry region in the most narrow pore which can accommodate a He molecule ($H_{in} = 2.6$ Å). In a slightly wider pore ($H_{in} = 3.6$ Å), in which the adsorption of larger molecules (N_2, Ar) may occur, the density of He exceeds its bulk value by 22 times (25 in the Henry region). The He density approaches its bulk value in the wide mesopores ($H_{in} > 100$ Å). The ratio $\bar{\rho}/\rho_{f,He} = H_{He}/H_{in}$ sharply decreases with the pore size in the micropore range (3.6 Å < H_{in} = <20 Å) and then approaches unity as

$$\frac{\bar{\rho}}{\rho_{f,He}} = \frac{H_{He}}{H_{in}} \approx 1 + \frac{2B^s_{sg,He} + \sigma_{cc}}{H_{in}} = 1 + 27.2/H_{in} \quad (40)$$

(see Figure 4 and Table 2). Equation 40 gives a good estimate in the mesopores of width $H_{in} > 20$ Å, where the opposite wall potentials do not overlap. In these pores, the adsorption at the pore walls is the same as that at the open surface and follows the Henry law (eq 29). Deviations from the Henry isotherms are observed only in the extremely narrow micropores of width $H_{in} < 5$ Å.

(35) Weeks, J. D.; Chandler, D.; Andersen, H. C. *J. Chem. Phys.* **1971**, *54*, 5237.
(36) Rigby, M.; Smith, E. B.; Wakeham, W. A.; Maitland, G. C. *The Forces Between Molecules*; Clarendon Press: Oxford, 1986.
(37) Steele, W. A. *J. Phys. Chem.* **1978**, *82*, 817.
(38) Derderian, E. J.; Steele, W. *J. Chem. Phys.* **1971**, *55*, 5795.
(39) Vidali, G.; Cole, M. W. *Phys. Rev. B* **1984**, *29*, 6376.

Table 2. Various Definitions of the Pore Widths, the Solid−Gas Second Virial Coefficients, and the Influence of He Adsorption on the Calculated Excess Adsorption Isotherms

pore size center−center, H_{cc}, Å	5	5.5	6	6.5	7	8	9	10	13	20	40	100
geometrical pore size, H_{in}, Å	1.6	2.1	2.6	3.1	3.6	4.6	5.6	6.6	9.6	16.6	36.6	96.6
$B^s_{sg,Henry}$ at 77.4 K,[a] Å	−2.49	11	55.9	55.9	40.9	23.5	17.4	14.8	12.6	12	11.9	11.9
H_{He}, at 77.4 K and 0.1 MPa,[b] Å	0.03	26.6	102.1	102.8	80.2	52.2	42.6	38.8	37.7	43.4	63.2	123
$H_{He,Henry}$ at 77.4 K,[c] Å	0.02	27.5	117.8	118.4	88.8	55	43.7	39.7	38.2	44	63.8	123.8
$B^s_{sg,Henry}$ at 308 K,[d] Å	−2.41	−1.94	−1.34	−1.04	−0.921	−0.875	−0.876	−0.879	−0.876	−0.865	−0.856	−0.855
H_{He} at 308,[e] Å	0.18	1.61	3.32	4.43	5.16	6.25	7.25	8.24	11.3	18.3	38.3	98.3
(H_{He} at 77.4 K and 0.1 MPa)/H_{in}	0.02	12.67	39.25	33.17	22.28	11.35	7.61	5.88	3.93	2.61	1.73	1.27
(H_{He} at 308 K)/H_{in}	0.11	0.77	1.28	1.43	1.43	1.36	1.29	1.25	1.17	1.10	1.05	1.02
max. difference in the calculated excess adsorption isotherms of N_2 at 77 K,[f] %	n/a	n/a	−109.4	−17.54	−12.58	−6.68	−3.60	−2.37	−1.45	−0.83	−0.1	n/a
max. difference in the calculated excess adsorption isotherms of CH_4 at 308 K,[g] %	n/a	n/a	−21.61	−6.01	−5.21	−5.48	−5.20	−4.20	−3.20	−2.90	−3.05	−3.07

[a] The solid−gas second virial coefficient. Calculated from eq 42 at 77.4 K. [b] He pore size. Calculated from eq 43 at 77.4 K and 0.1 MPa. [c] He pore size determined from the Henry region. Calculated from eq 44 at 77.4 K. [d] The solid−gas second virial coefficient. Calculated from eq 42 at 308 K. [e] He pore size determined from the Henry region. Calculated from eq 44 at 308 K. [f] Between isotherms calculated with H_{He} (at 77.4 K and 0.1 MPa) and H_{in} at $P/P_0 = 1$. [g] Between isotherms calculated with H_{He} (at 308 K) and H_{in} at $P = 4.84$ MPa.

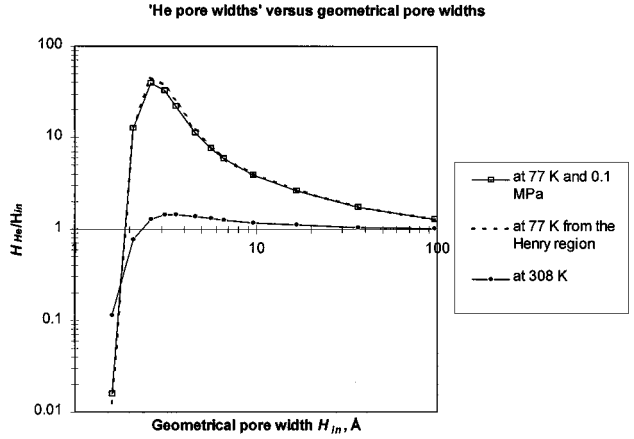

Figure 4. Ratio of the He calibrated pore widths, H_{He} (eq 43), to the geometrical (internal) pore widths, H_{in}. Dotted lines are He pore widths calculated from the Henry region, $H_{He,Henry}$ (eq 44), at 77 K. At 308 K, H_{in} is identical to $H_{He,Hnery}$.

In the micropores of width 5 Å < H_{in} < 20 Å, isotherms are practically linear and follow the Henry approximation (eq 21):

$$\bar{\rho} = \left(1 + \frac{2B^s_{sg,He} + \sigma_{cc}}{H_{in}}\right)\rho_{f,He} \qquad (41)$$

Therewith, the solid−gas second virial coefficient, $B^s_{sg,He}$, in micropores is greater than that for the open surface (eq 28) and depends on the pore width:

$$B^s_{sg,He} = \frac{1}{2}\int_0^H [\exp[-U_{ext,He}(z)/k_BT] - 1]\, dz \qquad (42)$$

The solid−gas second virial coefficients calculated from eq 42 are presented in Table 2. In Figure 5 we plot the solid−gas second virial coefficients of He in a set of pores at different temperatures. At low temperatures, $B^s_{sg,He}$ (H_{in}) exhibits a sharp maximum corresponding to pores of the order of the molecular diameter of He. With an increase in pore size, $B^s_{sg,He}$ (H_{in}) decreases rapidly, and in wider pores, it is almost a constant and depends on temperature only. With the increase in temperature, the maximum in $B^s_{sg,He}$ (H_{in}) gradually diminishes and disappears at temperatures greater than ca. 300 K. The Boyle point occurs at 220 K, when $B^s_{sg,He}$ (H_{in}) ≈ 0. Above 220 K the carbon−He second virial coefficients are negative in all pores.

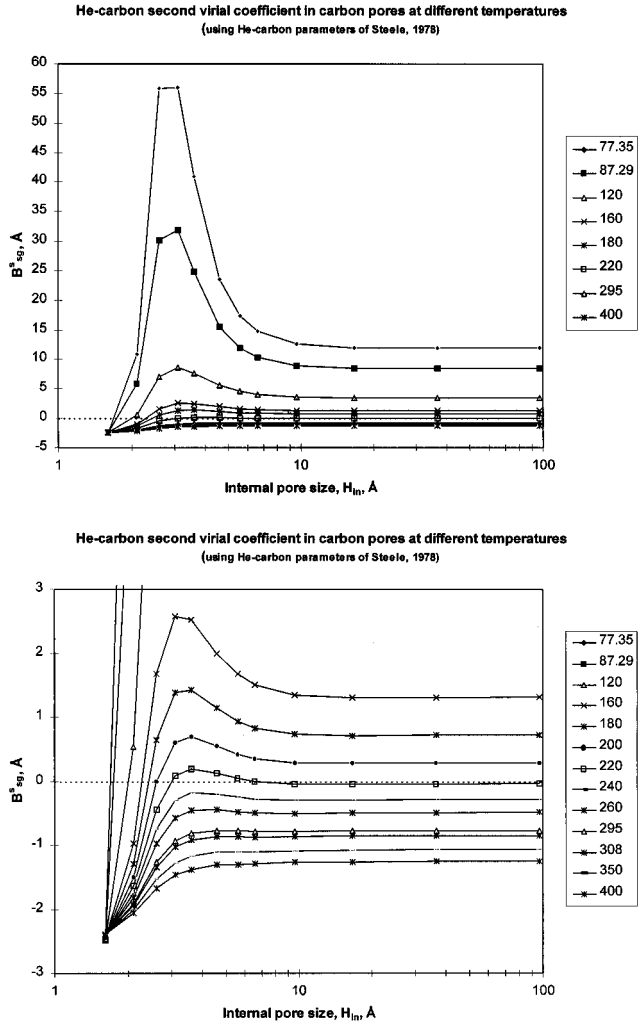

Figure 5. Solid−gas second virial coefficients of He in carbon slit pores at different temperatures. Calculated from eq 42. In the bottom half, the region around $B^s_{sg} = 0$ is expanded. Temperature in Kelvin.

The He calibrated pore widths, H_{He} (eq 18), were calculated as

$$H_{He} = \int_0^H \rho_{He}(z)\, dz/\rho_{f,He} = \frac{\bar{\rho}}{\rho_{f,He}} H_{in} \qquad (43)$$

To mimic the experimental determination of the adsorp-

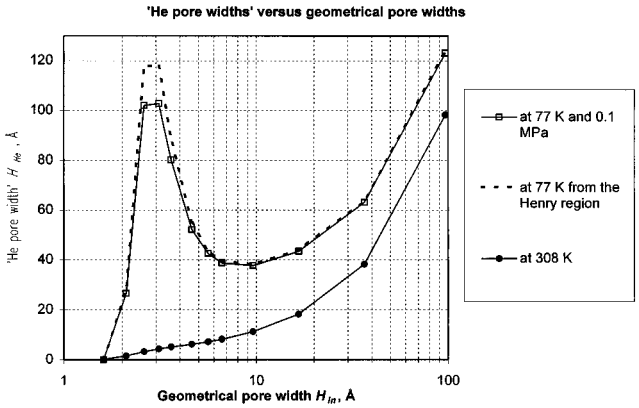

Figure 6. He calibrated pore widths, H_{He} (eq 43), versus the geometrical (internal) pore widths, H_{in}. Dotted lines are He pore widths calculated from the Henry region, $H_{He,Henry}$ (eq 44), at 77 K. At 308 K, H_{He} is identical to $H_{He,Henry}$.

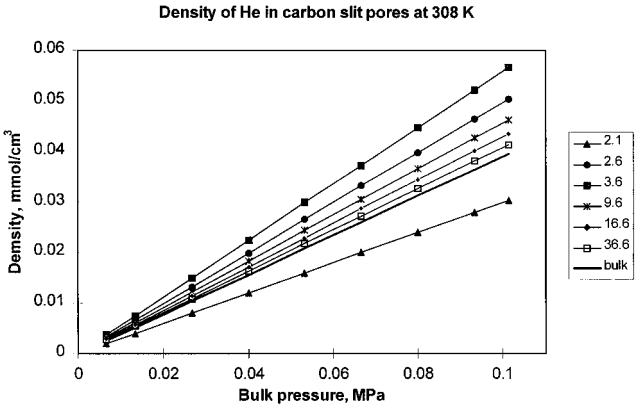

Figure 7. NLDFT absolute adsorption isotherms of He in carbon micropores at 308 K. The density of He has been calculated from eq 39. Pore sizes are internal, H_{in}.

tion volume, the He calibrated pore widths were calculated using a single point of the NLDFT isotherms, namely at 0.1 MPa. The He calibrated pore widths were also calculated from the Henry regions of isotherms (eq 23) as

$$H_{He,Henry} = \int_0^H \exp[-U_{ext,He}(z)/k_B T]\, dz = \left(1 + \frac{2B^s_{sg,He} + \sigma_{cc}}{H_{in}}\right) H_{in} \quad (44)$$

The results for a set of pores in the range of widths H_{in} = 1.6−96.6 Å are presented in Table 2 and Figure 6. The He calibrated pore width determined at 77 K is a nonmonotonous function of the internal pore width with a prominent maximum in the range of molecular sizes. This effect diminishes with the increase of temperature.

In the extremely narrow pore (H_{in} = 1.6 Å), which cannot accommodate He molecules, He adsorption and, consequently, the He pore width are almost zero. For the slightly wider pore (H_{in} = 2.1 Å), the He pore width is 26.6 Å. The maximum of the He calibrated pore width corresponds to the pore within which the potentials from the opposite pore walls overlap so vigorously that the two minimums become unsplit. Maximum values (H_{He} = 102−103 Å) are obtained for pores of H_{in} = 2.6 Å and H_{in} = 3.1 Å. As the pore size increases, the potential from the pore walls exhibits two minimums; He adsorption decreases to the minimum value characteristic of an open surface. Therewith, $B^s_{sg,He}$ approaches the open surface value (eq 28). Consequently, the He pore size decreases and passes through the minimum in the pore of H_{in} = 9.6 Å. In wider pores, the He pore size increases linearly according to the asymptotic relation (eq 40). In wide mesopores, the He calibrated pore width is 27.2 Å greater than the geometrical pore width; *e.g.*, in the pore of H_{in} = 96.6 Å, H_{He} = 123.8 Å.

The dotted line in Figure 6 shows the He calibrated pore widths, $H_{He,Henry}$, calculated from the initial Henry regions of He isotherms. Qualitatively, they correspond to the He pore widths determined from adsorption at 0.1 MPa, H_{He}; however, the pore widths derived from the Henry regions are always larger. Significant deviations occur in the sub-nanometer pores (H_{in} < 10 Å), in which He adsorption does not obey the Henry law. In the wider pores, the He pore widths determined from the Henry law agree with those calculated from the full isotherm to within 1% (see also Table 2).

We note that, in all the pores (except the extremely narrow pore of H_{in} = 1.6 Å, in which adsorption cannot occur), the ratio of the He calibrated pore width to the geometrical pore width (H_{in}) is always significantly greater than unity and the maximum corresponds to the pore of H_{in} = 3.1 Å. In this case the He pore width is 33 times bigger than the geometrical pore width. The He pore width calculated from the Henry law for this pore size is 38 times bigger than the geometrical internal pore width (Figure 4).

V.2. He Adsorption at 308 K. Adsorption of He at 308 K is very weak. The calculated isotherms are linear (Figure 7) and obey Henry's law (eqs 26 and 40). The maximum density is achieved in the pore of H_{in} = 3.6 Å. The solid−gas second virial coefficient (eq 28), $B^s_{sg,He}$, has been estimated as −0.85 Å. Note that $B^s_{sg,He}$ is negative; that is, 308 K is above the Boyle point temperature (Figure 5).

Since the He adsorption at 308 K occurs in the Henry region, the He calibrated pore widths, H_{He} and $H_{He,Henry}$, calculated from eqs 43 and 44, respectively, are identical. They exceed the internal pore widths, H_{in}, by ca. 1.69 Å, and the difference gets smaller with the decrease in pore size and even becomes negative in extremely narrow pores of H_{in} = 2.1 Å (see Table 2). However, in the narrowest pores of H_{in} < 5 Å, even this small difference leads to a non-negligible contribution to the excess adsorption of supercritical species at high pressures. This effect will be illustrated below with the example of methane adsorption.

V.3. Boyle Temperature of He Adsorption. In Figure 5 we plotted the solid−gas second virial coefficients of He in a set of pores at different temperatures, from which it follows that the Boyle point of He occurs at ca. 220 K. We have performed additional calculations of $B^s_{sg,He}(T)$ with three different sets of parameters for the C−He intermolecular interactions (Figure 8). In addition to the C−He parameters of Steele,[37] which are adopted throughout this work, the parameters of Vidali and Cole[39] (ϵ_{sf} = 16.2 K, σ_{sf} = 2.74 Å) and also the parameters calculated from the combining rules (ϵ_{sf} = 17.07 K, σ_{sf} = 3 Å) were chosen to demonstrate that the Boyle point is observed at temperatures from 200 to 240 K (at 220 K using the parameters of Steele). The Boyle point temperature of He adsorption in micropores (the virial coefficients calculated from eq 42) is insensitive to the pore size and differs insignificantly from that corresponding to an open surface.

Performing the He calibration at the Boyle point seems to be a natural solution for diminishing the discrepancies between the theoretical and experimental definitions of excess adsorption.[20] Steele estimated the Boyle point of He on carbon as 290 K. However, our calculations indicate that the Boyle point for this system lies in the range 200−

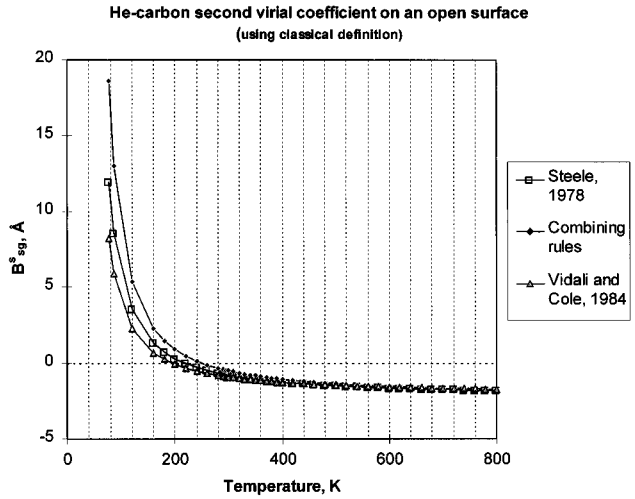

Figure 8. Temperature dependence of the carbon−He solid−gas second virial coefficient on an open surface. Calculated from eq 42, for a wide slit pore of H_{cc} = 100 Å (equivalent to eq 28). Different symbols denote different parameters of carbon−He interactions (see text).

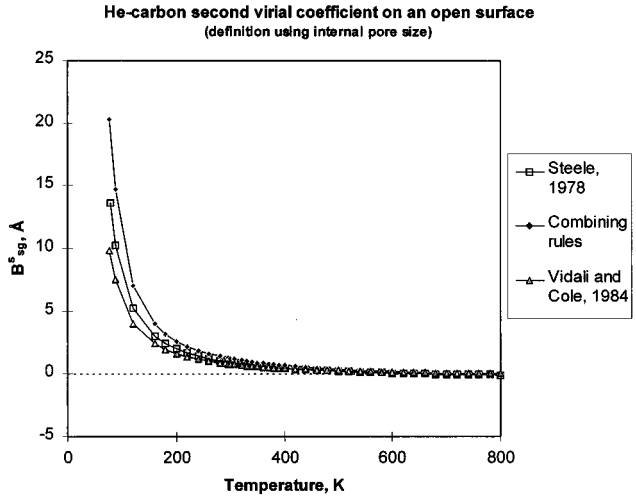

Figure 9. Same as Figure 8 but using the internal geometrical definition of the pore width, H_{in} (eq 45).

240 K; *i.e.*, it is lower than ambient temperature. At ambient temperature, the solid−gas second virial coefficients of He are negative (Figures 5a and b and 8), making the He pore width smaller than the nominal pore width, H_{cc}, used in the classical definition of the solid−gas virial coefficient (eqs 28 and 42).

A reasonable alternative is to define the solid−gas second virial coefficient using the internal pore width, H_{in}, instead of the nominal pore width, H_{cc}:

$$B^s_{sg,He} = \frac{1}{2}[\int_0^H \exp[-V_{ext,He}(z)/k_BT]\,dz - H_{in}] \quad (45)$$

The Boyle point defined thereby is shifted to higher temperatures. Indeed, the virial coefficients calculated from eq 45 are *almost* zero at elevated temperatures (Figure 9). The Boyle point is ca. 660 K, and at higher temperatures $B^s_{sg,He}(T)$ is only slightly negative and decreases very slowly. Thus, the pore volume determined with He at the Boyle point, defined through eq 45, would be equal to the geometrical internal pore volume, V_{in}. Virtually, this is equivalent to the He calibration in the high-temperature limit. The definition (eq 45) is consistent with the requirement of setting the pore boundaries provided zero excess mass/volume of solid. In these considerations, the thermal expansion of the solid at high temperatures is neglected.

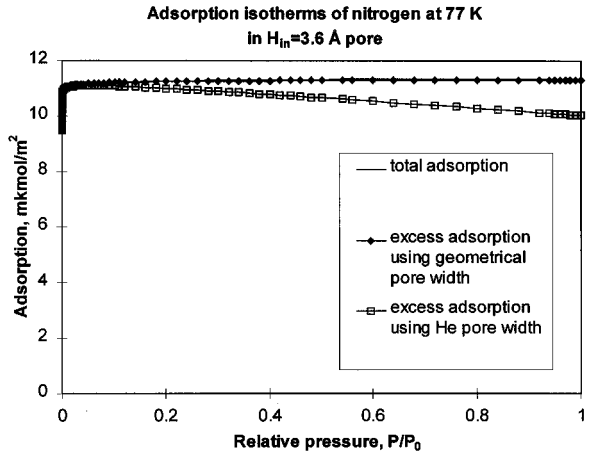

Figure 10. Comparison of the NLDFT N_2 excess adsorption isotherms in a slit micropore at 77.4 K calculated with the geometrical, H_{in}, and helium, H_{He}, pore widths. The He pore width has also been calculated at 77.4 K (eq 43).

VI. Calculations of Excess Adsorption Isotherms in Carbon Micropores

VI.1. Vapor Adsorption. N_2 at 77 K. Nitrogen isotherms in carbon slit pores at 77 K were calculated by means of the NLDFT model (eqs 34−37). Since the bulk gas density is small, the excess isotherms calculated using various geometrical definitions of the pore width (H_{cc} or H_{in}) are practically indistinguishable and very close to the absolute adsorption isotherm. At the same time, the He calibrated excess adsorption (eq 19b), calculated based on the He pore width, H_{He} (eq 43), differs considerably from the excess adsorption calculated with the use of the geometrical definitions of the pore size (see Table 2). The maximum differences (at $P/P_0 = 1$) are −12.6% for the H_{in} = 3.6 Å pore and −17.5% for the H_{in} = 3.1 Å pore (see Figure 12). In the extremely narrow pore of H_{in} = 2.6 Å, in which the absolute adsorption of nitrogen is very small, the difference is even −109%. The absolute and excess isotherms per unit area in the H_{in} = 3.6 Å pore are presented in Figure 10.

In the molecular size pores, the He calibrated excess adsorption isotherms of N_2 are not monotonous. They pass through the maximum and then decrease at high relative pressures. To the best of our knowledge, no such isotherms have been published. This may be explained that, in real materials, adsorption on the external surface of particles masks this effect. The following estimate confirms this hypothesis. The standard N_2 adsorption on nonporous solids at relative pressure $P/P_0 = 0.7$ is ca. 21 mkmol/m^2.[40] The He calibrated excess N_2 adsorption in a 4 Å slit pore at the same relative pressure is ca. 10 mkmol/m^2. It may be assumed that even, in perfect microporous materials, at least 5% of the total surface area may be accounted for by the external surface area, on which multilayer adsorption occurs. In this case, the contribution of adsorption on the external surface would be ca. 10% and could compensate for the decrease of the excess isotherms in micropores.

VI.2. Implications for the Characterization of Microporous Solids. The He calibration may affect the determination of the mesopore surface area from the comparative or α−*S* plots. For example, the experimental (i.e. He calibrated) isotherm on micro-mesoporous material

(40) Gregg, S. J.; Sing, K. S. W. *Adsorption, Surface Area and Porosity*; Academic Press: New York, 1982.

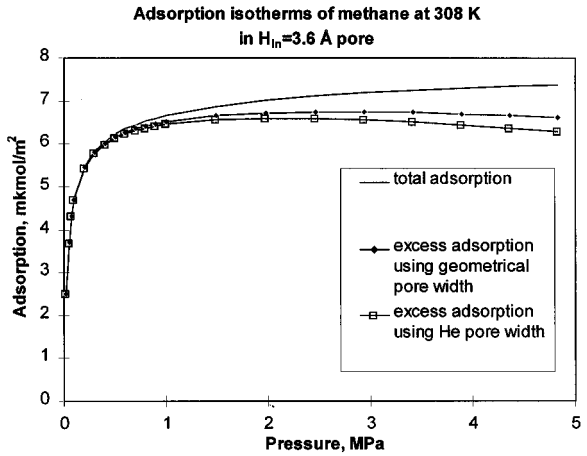

Figure 11. Comparison of the NLDFT CH_4 excess adsorption isotherms in a slit micropore at 308 K calculated with the geometrical, H_{in}, and helium, H_{He}, pore widths. The He pore width has also been calculated at 308 K (eq 43).

is often expressed as a sum of two isotherms (in the micropores and on the surfaces of the mesopores) as

$$N_{abs} = N_{micr} + \alpha_{std} S_{meso} = V_{micr}\rho_L + \alpha_{std} S_{meso} \quad (46)$$

Here, α_{std} is the standard adsorption on an open surface per unit area, S_{meso} is the surface area of the mesopores, and V_{micr} is the volume of the micropores, determined assuming that the adsorbate density equals the bulk liquid density ρ_L. Herewith, the isotherm in micropores is supposed to be of Type I, according to IUPAC classification,[40] with a horizontal plateau as $P/P_0 \rightarrow 1$. If the He calibrated isotherms in micropores were nonmonotonous, the surface area of the mesopores would be underestimated and, subsequently, the micropore volume would be overestimated.

The NLDFT calculated isotherms in model pores are employed now for calculating pore size distributions (PSDs) from the low-temperature nitrogen and argon adsorption isotherms.[25−31] Because the theoretical isotherms are compared with the He calibrated experimental isotherms, the former should also be He calibrated. The He calibration of the model pores and theoretical excess isotherms will ensure self-consistency of theory and experiment. These considerations require further investigation.

VI.3. Supercritical Adsorption. CH_4 at 308 K. The NLDFT calculated CH_4 adsorption isotherms at 308 K are presented in Figure 11. In the micropores of molecular sizes, at pressures up to 5 MPa the difference between the He calibrated excess isotherm (eq 19b) and conventional excess isotherms, calculated using the internal pore width, H_{in}, is of the same order as the difference between the latter and the absolute adsorption isotherm. At higher pressures (not calculated here), the discrepancies between different excess adsorption isotherms would be greater, and the Bering point[41] (where the excess adsorption is zero) would occur at lower bulk pressure. Note that, in this example, the theoretical He calibration has been carried out also at 308 K. At this temperature and normal atmospheric pressure, He adsorption is hardly measurable and, therefore, is commonly neglected.

In Figure 12, the deviations in the excess adsorption isotherms calculated by using various definitions of the pore width are plotted. It is worth noting that, for N_2 adsorption at 77 K, the error vanishes as the pore width increases, while in the case of supercritical adsorption (CH_4 at 308 K) there is a constant error of the order of 3% because of a high bulk density.

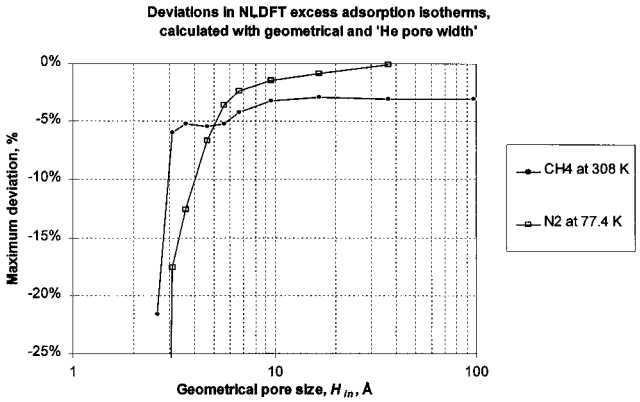

Figure 12. Maximum deviations in the NLDFT excess adsorption isotherms in carbon slit pores, calculated with the geometrical, H_{in}, and 'He' definitions for the pore width (eq 43). For N_2 at 77 K the maximum deviations have been calculated at $P/P_0 = 1$, and for CH_4 at 308 K, they have been calculated at $P = 4.84$ MPa. Note that the maximum deviation of −109% for N_2 isotherms in pore $H_{in} = 2.6$ Å is not shown.

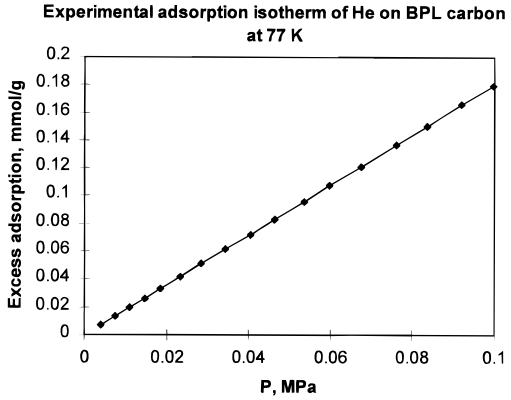

Figure 13. Experimental excess adsorption isotherm of He on BPL carbon at 77.4 K.

VII. Experimental Section. He Adsorption on BPL Carbon at 77 K

To get experimental support for our theoretical calculations of He adsorption presented in this work, we have measured He adsorption on BPL carbon at 77.4 K. The excess adsorption isotherm was measured manually with the volumetric setup Autosorb-1C (Quantachrome Corp.).

First, the volume of an empty sample cell was determined by He expansion from a known calibrated volume. The volume of the 'cold' part of the sample cell, which is immersed in the liquid nitrogen during the measurements at 77 K, was also determined. Then, 1.36 g of BPL carbon was placed in a sample cell, and the cell was outgassed at 300 °C overnight. Assuming that He adsorption at ambient temperature (295 K) is small (see Figure 5 with the solid−gas second virial coefficients for He), a true density of the BPL carbon was determined as 2.13 g/cm^3. This value coincides well with the density of amorphous carbon (ca. 2.0 g/cm^3) and the density of graphite (2.26 g/cm^3).[42]

The adsorption isotherm at 77 K was measured manually up to normal atmospheric pressure. At each point, equilibrium was reached in ca. 10−20 min. The adsorption points were calculated using the ideal gas law.

The experimental isotherm is presented in Figure 13. The isotherm is almost linear. The amount adsorbed at normal atmospheric pressure is $N_{ex} = 0.179$ mmol/g. Such quantities

(41) Bering, B. P.; Zhukovskaja, E. G.; Rakhmukov, B. Kh.; Serpinski, V. V. *Izv. Akad. Nauk SSSR, Ser. Khim.* **1967**, 1656; **1967**, 1662; **1968**, 30.

(42) Robertson, J. *Adv. Phys.* **1986**, *35*, 317.

are measurable with the modern adsorption instruments, capable of measuring micromoles. This confirms that when He is used for the determination of the adsorption volume at 77 K, He adsorption is significant and cannot be neglected.

We have estimated the surface area of the BPL carbon using the method developed by Steele and Halsey.[16,17] Since the He adsorption obeys the Henry law, the excess adsorption per unit area is described by eq 29. The surface area is then calculated as

$$S = \frac{N_{ex}}{B^{s}_{sg,He}\,\rho_{f,He}} \tag{47}$$

Using the theoretical solid−gas second virial coefficient of He on an open surface at 77.4 K (11.9 Å) and the bulk density at 760 Torr of 0.157 mmol/cm^3, the surface area of BPL carbon turns out to be 957 m^2/g.

The pore volume of BPL carbon is ca. 0.5 ± 0.02 cm^3/g, as determined from a variety of methods. Using the slit pore model, the average pore width can be estimated as

$$\bar{H} = \frac{2V_{pore}}{S} \tag{48}$$

The average pore width, estimated through eq 47, is 10.4 Å. In such a pore, the solid−gas second virial coefficient of He is ca. 12.6 Å, i.e. slightly bigger than $B^{s}_{sg,He}$ on an open surface, the value used in the Steele−Halsey method (eq 47). With $B^{s}_{sg,He}$ = 12.6 Å in eq 47, the surface area of BPL would be 903 m^2/g, in very close agreement with the results of nitrogen measurements and also with our preliminary calculations of the surface area of BPL carbon from nitrogen adsorption at 77 K based on the NLDFT model.[43] These results will be presented elsewhere.

VIII. Conclusions

The inconsistency of the experimental and the theoretical adsorption isotherms has been analyzed. It is shown that the experimental calibration on the one hand and the ambiguousness in the theoretical pore boundary settings on the other hand may lead to substantial discrepancies between the experimental and the theoretical excess isotherms. A new definition of the excess adsorption is proposed for use in the molecular models of adsorption. This definition is based on the calibration of the theoretical models in a manner which mimics the experimental calibration procedure.

The method of theoretical calibration has been developed on the example of helium calibration. The notions of the He calibrated pore volume and the He calibrated pore size have been introduced, and the He calibrated theoretical excess isotherms have been defined. This definition of the excess adsorption is independent of the pore boundary settings. The proposed method diminishes the discrepancies between the theoretical and the experimental excess adsorption isotherms and makes the theory and the experiment entirely consistent.

The quantitative estimates have been made by means of the nonlocal density functional theory (NLDFT) applied to the adsorption of He, N_2, and CH_4 in the micropores of active carbons at liquid nitrogen and ambient temperatures. It has been shown that the average density of He confined in the sub-nanometer pores may exceed the bulk density by tens of times. The He density and the He calibrated width of the slit-shaped carbon micropores are nonmonotonous functions of the pore geometrical width and attain their maximum values in the molecular size pores.

On the basis of the NLDFT calculations of the He and N_2 adsorption in microporous carbons, it is shown that when the experimental He calibration is carried out at 77 K, the N_2 adsorption isotherms in the sub-nanometer pores may be seriously unprecise in the high-pressure region. The nonmonotonous excess isotherms in the smallest pores have been predicted. Even when the He calibration is performed at ambient temperature, the theoretical and experimental excess isotherms of supercritical CH_4 deviate significantly, and the error does not vanish as the pore size increases.

Because of high bulk densities, the theoretical excess adsorption isotherms of supercritical fluids strongly depend on the chosen definition of the pore volume. The proposed method of the theoretical calibration reduces the discrepancies between the theoretical and the experimental isotherms of supercritical fluids and allows us to avoid ambiguousness in the pore boundary settings.

The theoretical predictions of He adsorption are in qualitative agreement with the experimental isotherm measured on the BPL active carbon at 77 K.

The theoretical calibration is recommended for adjusting any molecular model of adsorption phenomena, such as density functional theory, molecular dynamics, and grand canonical and other Monte Carlo simulations.

Appendix

After this paper had been completed, Malbrunot *et al.*[44] published several prominent experimental examples which support its main idea. The authors[44,45] measured adsorption of simple gases at ambient temperature (298 K) and very high pressures (up to 650 MPa). Under such conditions, the bulk fluid density is so large (of the same order as the density of the adsorbate in pores) that the excess adsorption isotherms become extremely sensitive to the definition of the reference fluid volume, V_f, used for calibration of the experimental data. Minor variations in V_f lead to significant shifts in the excess adsorption and may even change its sign and the shape of the isotherm. This makes the problem of calibration critical. Malbrunot *et al.* have found earlier[45] that, while determining V_f by means of He calibration at ambient temperature, the excess adsorption isotherms of Ar, CH_4, Kr, N_2, and Ne on microporous activated carbon passed through zero at a certain pressure and became negative. The conditions at which the excess adsorption becomes zero are referred to as the Bering point.[41] However, while performing the He calibration at 673 K,[44] the recalculated excess isotherms were everywhere positive.

To illustrate this effect, we have performed the NLDFT calculations of N_2 adsorption in the carbon slit-shaped pores at 298 K. Nitrogen was modeled using the parameters listed in Table 1, except for the diameter of hard spheres, d_{HS} = 3.467 Å, which was calculated from the Barker−Henderson formula.[46] It was found that these parameters provide a very good correspondence of the theoretical and experimental properties of the bulk N_2 based on the high-pressure−density data given in ref 47.

In Figure 14, we present a qualitative comparison of the NLDFT excess N_2 isotherms at 298 K with the experimental excess isotherm on the activated carbon GAC-250 measured by using He calibration at room temperature.[45] Three theoretical excess isotherms in a slit pore with the internal (geometrical) pore width H_{in} = 9.6 Å were calculated by using different reference fluid volumes corresponding to (1) the geometrical pore width H_{in} = 9.6 Å, (2) the He calibrated pore width, H_{He} = 11.38

(43) Neimark, A. V.; Ravikovitch, P. I. Unpublished.

(44) Malbrunot, P.; Vidal, D.; Vermesse, J.; Chahine, R.; Bose, T. K. *Langmuir* **1997**, *13*, 539.
(45) Malbrunot, P.; Vidal, D.; Vermesse, J.; Chahine, R.; Bose, T. K. *Langmuir* **1992**, *8*, 577.
(46) Barker, J. A.; Henderson, D. *J. Chem. Phys.* **1967**, *47*, 4714.
(47) Vermesse, J.; Vidal, D.; Malbrunot, P. *Langmuir* **1996**, *12*, 4190.

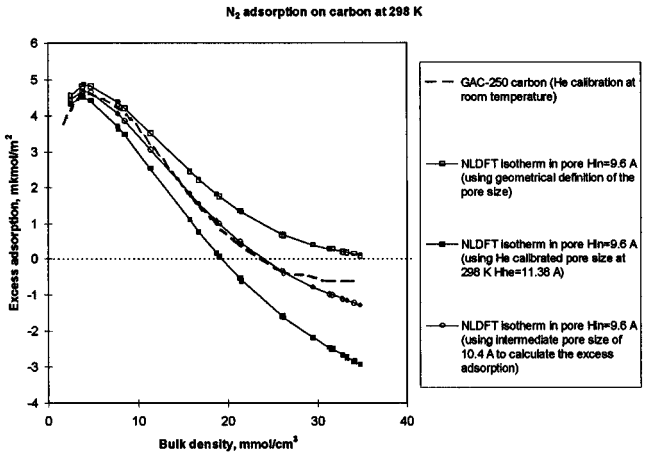

Figure 14. Excess adsorption isotherms of N_2 at 298 K at high pressures (see text in the Appendix). The experimental isotherm on activated carbon[45] has been normalized to the maximum amount adsorbed, which corresponds to the specific surface area of 860 m^2/g. S_{BET} = 1030 m^2/g.[44]

Å, determined at 298 K (eq 44), to match the temperature at which the He calibration was performed in the experiment, and (3) an intermediate pore width of 10.4 Å.

Although the difference among the reference pore widths is quite small, the difference in the isotherms is significant. The excess adsorption calculated by using the geometrical pore width is positive in the range of bulk pressures up to ca. 35 mmol/cm^3, while the excess adsorption calculated by using the He calibrated pore width at 298 K becomes negative at a bulk density of ca. 19 mmol/cm^3. The position of the experimental Bering point (23−24 mmol/cm^3) is in agreement with the theoretical excess isotherm calculated by using 10.4 Å as the reference pore width (Figure 14). The experimental excess isotherm, recalculated by employing the He calibration at 673 K,[44] is close (in the range of bulk pressures up to ca. 25 mmol/cm^3) to the theoretical excess isotherm, calculated by the geometrical pore width, which could be expected because the use of the geometrical pore width for calibration implies that the He adsorption is negligible. The comparison of the theory and the experiment, presented in Figure 14, is regarded as a qualitative one because, firstly, we did not account for a possible pore size heterogeneity of the carbon GAC-250 and, secondly, we used the model parameters for the fluid−solid interactions, which may need a correction for this particular sample.

Acknowledgment. This work has been supported in part by the TRI exploratory research program. Quantachrome Corp. is acknowledged for a free loan of the Autosorb-1-C sorbtometer.

LA970266S